

# RECENT DEVELOPMENT STATUS OF HIGH STRENGTH LINEPIPE STEELS FOR SOUR SERVICE

H.G. Jung, W.K. Kim, K.K. Park and K.B. Kang

Technical Research Laboratories, POSCO,  
1 Geodong-dong, Nam-gu Pohang 790-785 Gyungbuk, Republic of Korea

Keywords: High Strength Linepipe, Sour Service, HIC, SSC, X80, Mechanical Properties, Charpy Toughness, NACE, Pipe Forming

## Abstract

POSCO is involved in efforts to produce superior linepipe steels for sour service and to develop high strength linepipe steels for sour service. Several experimental trials involving multiple process variables have been performed to enhance the mechanical properties and HIC/SSC resistance of high strength linepipe steels. Results after ERW pipe forming of API X80 hot strip show that an increase in the t/D ratio increases the sensitivity to hydrogen cracking mechanisms, such as HIC. The increased dislocation density resulting from pipe forming can increase the diffusible hydrogen content. This paper summarizes the effect of pipe forming on the sour resistance of high strength linepipe steels.

## Introduction

Recently, the number of new H<sub>2</sub>S containing oil and gas wells has increased compared to conventional wells. This is due to the consumption of sweet wells during the last decades. As well as unconventional resources such as shale gas and hydrate, development of more sour wells is required to meet the worldwide demand for oil and gas expected in future. Between 15 and 25% of natural gas resources in the U.S. may contain H<sub>2</sub>S, while worldwide the figure could be as high as 30% [1].

When linepipe steels are exposed to H<sub>2</sub>S gas, high resistance to sour corrosion is very important because of hydrogen related problems such as HIC and SSC. Both HIC and SSC belong to hydrogen degradation phenomena.

Unlike HIC which occurs under conditions without an applied stress, SSC occurs under externally or internally stressed or strained conditions and propagates perpendicularly to the direction of tensile stress. The hydrogen atoms generated by a sulphide corrosion process are adsorbed on the steel surface and diffuse into the steel. In steel, hydrogen atoms diffuse to regions having a high triaxial tensile-stressed condition or to various defects such as inclusions, precipitates and dislocations that act as hydrogen trapping sites and cause degradation of the steel [2].

HIC is generally defined as cracking parallel to the steel rolling direction in the absence of an applied stress. Sometimes, HIC is termed stepwise cracking when the cracks are connected in the through thickness direction [3].

HIC is primarily associated with inclusions such as manganese sulphides or oxide clusters having voids around them. The cracking mechanism of HIC is generally explained by the internal hydrogen pressure theory, according to which a crack is initiated because of the formation of hydrogen pressure developed at internal voids such as at inclusion interfaces.

SSC is classified as either type I or type II. Type I SSC is termed stress oriented HIC (SOHIC) because of the formation of the HIC cracks parallel to the applied stress [4]. The cracking in type I SSC can be divided into two stages. The first stage is the formation of HIC parallel to the applied stress. In the second stage, the HIC cracks link together in a direction perpendicular to the applied stress. Type II SSC is recognized as cracking which results from typical hydrogen embrittlement. After introduction into the metal, hydrogen atoms diffuse to regions with a high triaxial stress field or to some microstructural features where they can be trapped and ultimately decrease the measured ductility of the metal. Atomic hydrogen trapped in steel lowers the cohesive bonding strength between Fe atoms and second phases within the tri-axial stress field and induces the embrittlement of the steel. The final failure occurs in a direction perpendicular to the applied stress by a quasi-cleavage mechanism. Specifying a maximum hardness of less than 248 HV has been required to prevent type II SSC [3,4].

POSCO is trying to supply superior API steels for sour service and to develop high strength grade sour service materials. In order to minimize the formation of MnS, which is detrimental in terms of HIC and SSC, sulphur content is strictly controlled to less than 10 ppm. Steel cleanliness and segregation control is optimised to prevent the development of HIC and SSC. POSCO has recently performed several experimental trials with several process variables to enhance the mechanical properties and HIC/SSC resistance of high strength linepipe steels. To study the effect of forming on the properties of hot coil and plate, the properties were evaluated after pipe forming.

### **Properties of High Strength Linepipe Steel for Sour Environment**

High strength hot strip for sour environment was produced through mill trials. The nominal chemical composition of the high strength linepipe steel is given in Table I. The heat was produced with very low sulphur and phosphorus levels and coils were produced at three thickness levels, namely 12, 16 and 18 mm.

For the three coils, mechanical properties and HIC/SSC resistance were investigated before pipe forming as presented in Table II. The results showed that strength met X80 requirements. The coils had high CVN values, over 300 J at -5 °C. The high CVN values of coils were not changed even at -60 °C. Hardness of the coils was measured using a load of 500 gf. The measured hardness values are less than 248 HV, which is the limiting Vickers hardness value for acceptable sour service. HIC tests were performed in NACE TM0284 Solution A for 96 hours. For all coils, CAR (crack area ratio) values were 0%. SSC tests were conducted using the 4 point bending test method of ASTM G39 for 720 hours. There was no failure of the 4 point bend specimens during the testing period. After the tests, no cracks were observed on the steel surface.

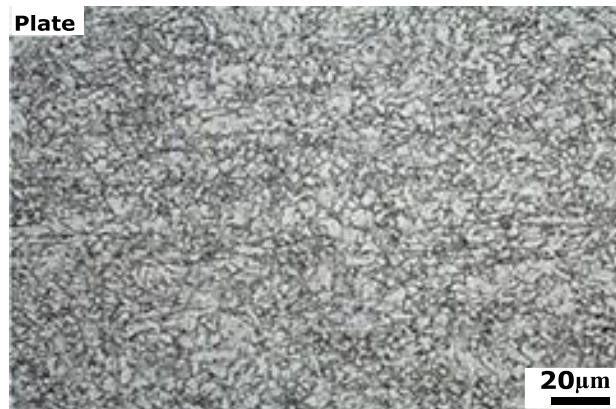
Table I. Nominal Chemistry of High Strength Hot Strips for Sour Service, wt.%

C	Mn	Si	P+S	Cu+Ni	Ca	Nb+Ti+V	Others
≤0.07	≤1.8	≤0.5	≤0.005	≤0.8	>0.002	≤0.2	Cr, Mo

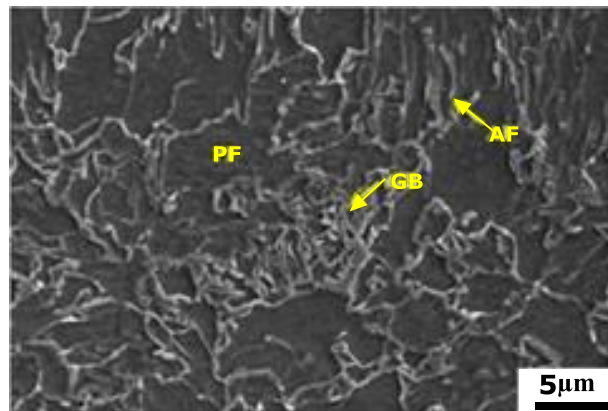
Table II. Mechanical Properties and HIC/SSC Resistance of Three Coils

Coil no.	Thick (mm)	YS (MPa)	TS (MPa)	YR (%)	El. (%)	CVN @ -5 °C, (J)	Hardness (HV)	HIC (CAR, %)	SSC (4 point)
HR12	12	582	633	92	35	341	196	0	No crack
HR16	16	563	625	90	39	498	191	0	No crack
HR18	18	561	653	86	40	485	189	0	No crack

A typical microstructure of the 12 mm thick steel is shown in Figure 1. In general, the microstructure consisted of homogeneous ferrite grains. However, as shown in Figure 1(b), the magnified view of an FE-SEM image reveals that the steel sheet microstructure was primarily composed of polygonal ferrite (PF) with a mixture of a small amount of acicular ferrite (AF) and granular bainite (GB).



(a) Lower Mag.



(b) Higher Mag.

Figure 1. Typical microstructure of the 12 mm steel sheet.

## Effect of Pipe Forming on the Mechanical Properties

The three coils were formed to 20 inch ERW pipe in a domestic pipe mill. The mechanical properties of each pipe were evaluated to observe the relationship between the coil and pipe properties. Specimens from the coiled strip and pipes respectively were obtained from the tail position of the coil and 180° position of the pipe where the welding line is at 0°. The effect of t/D ratio (thickness / diameter) on yield strength has been confirmed as shown in Figure 2.

For 12 mm pipe (t/D: 0.0236), the yield strength decreased by about 50 MPa compared to the coil. However, the yield strength of the 18 mm pipes (t/D: 0.0354) increased by about 30 MPa compared to that of the coils. These yield strength changes indicate that an increase or decrease in yield strength depends on the t/D ratio of the pipes. That is, the higher t/D ratio of the 18 mm thick pipes causes an increase in yield strength due to the work hardening after ERW pipe forming. Conversely, the lower t/D ratio of the 12 mm thick pipes results in a decreased yield strength because of the Bauschinger effect. The yield strength of the weld was over 560 MPa for both 12 mm and 18 mm pipes.

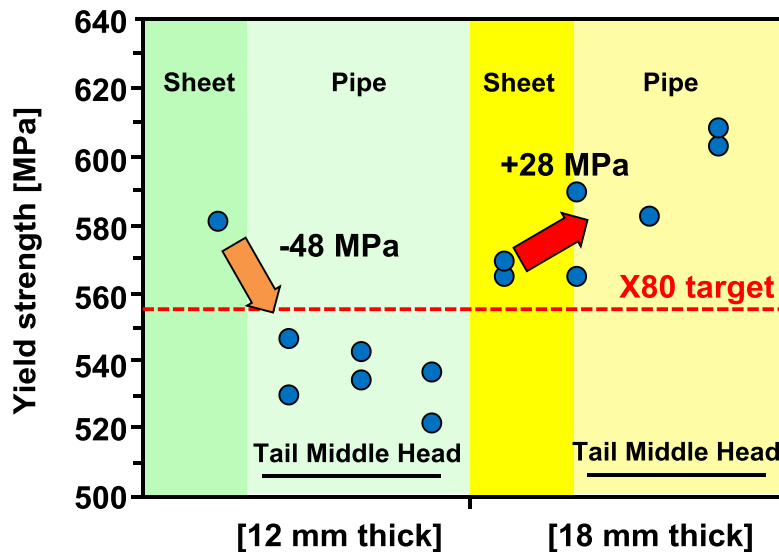


Figure 2. Yield strengths of the sheets and pipes with 12 mm and 18 mm wall thickness.

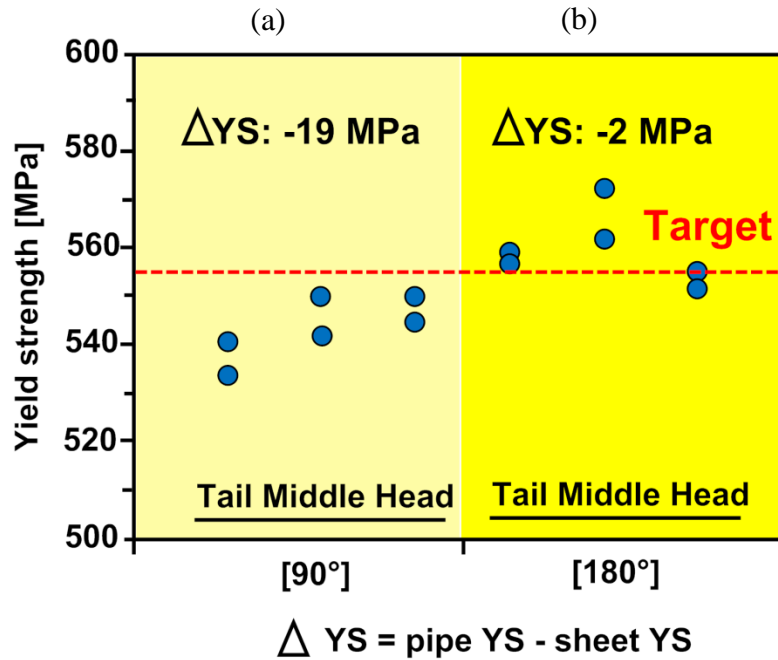


Figure 3. Yield strengths of the sheet and pipe with 16 mm wall thickness; (a) sheet, (b) pipe.

Figure 3 shows yield strengths of the sheet and pipe with 16 mm wall thickness. Unlike the 12 mm and 18 mm pipes, the yield strength change after pipe forming at the 180° position of the 16 mm pipe ( $t/D$ : 0.0315) is very small. This suggests that the yield strength is not changed after ERW pipe forming for mid level  $t/D$  ratios as for the 16 mm pipe. The neutral change in yield strength is likely to be due to the effects of Bauschinger and work hardening being approximately the same and cancelling each other out.

However, the yield strengths of the 16 mm pipe were different at the 90° and 180° positions as shown in Figure 3. That is, 180° position exhibits higher yield strengths than in 90° position. This means that more strain is accumulated at the 180° position of the ERW pipe as compared to the 90° position and thus yield strength increases due to work hardening.

Tensile strengths in sheets and pipes were almost the same. The tensile strengths of the coils and pipes met the target of grade X80, 625 MPa. The tensile strength of the weld was over 620 MPa for all pipes.

Regarding toughness, the CVN values of the pipes were almost the same as those in the coils as shown in Figure 4. CVN values were very similar along the length of the pipe, similar to the trend of tensile strengths. The high CVN values of coils and pipes did not change even at -60 °C. CVN values of weld were similar to those of the base materials.

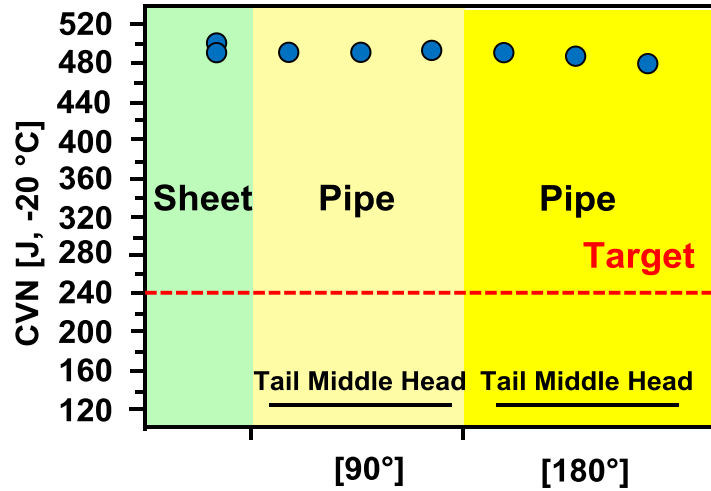


Figure 4. CVN values at -20 °C of the sheet and pipe with 16 mm thickness.

### Effect of Pipe Forming on the Sour Properties

The HIC test results of sheet and pipe, using NACE TM0284 Solution A, are presented in Figure 5 [5]. For the 12 mm thick specimen, no HIC was observed by ultrasonic inspection for either the sheet or pipe. No HIC was detected in the 18 mm thick steel sheet, however, HIC was detected in the 18 mm thick pipe which showed a different susceptibility to HIC depending on the pipe position. The average CAR value was 2.46% for the 180° position and 0.61% for the 90° position, meaning that the former position is almost 4 times higher than the latter as shown in Figure 5. Based on the HIC results, it is clear that the 18 mm thick pipe is more susceptible to HIC than the 12 mm thick pipe.

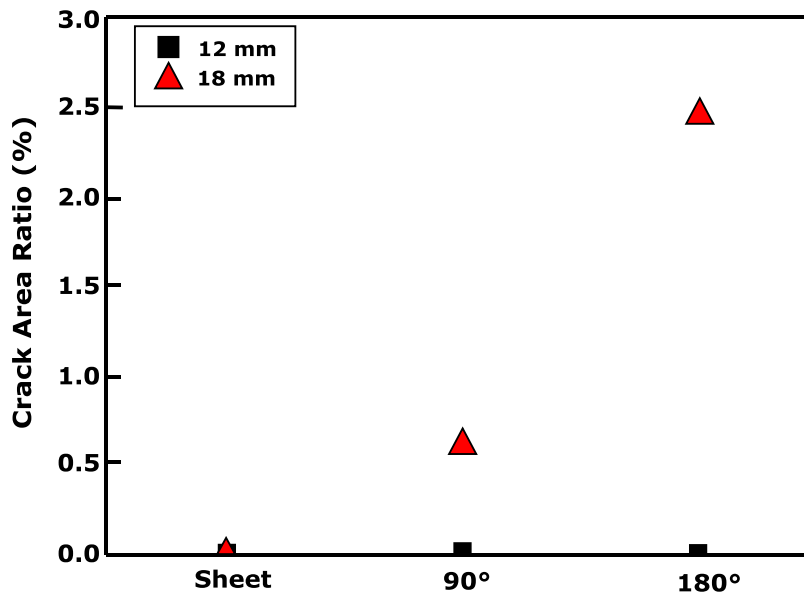


Figure 5. Average crack area ratio value (CAR) of sheet and pipe after HIC testing of 12 mm and 18 mm thick sheet and pipe.

After HIC testing, the amount of absorbed diffusible hydrogen was measured by the modified JIS Z3113 method and the results are presented in Figure 6. The diffusible hydrogen content was higher in the 18 mm thick steel than in the 12 mm thick steel and higher in the steel pipe than in the steel sheet, because the pipe has been plastically deformed by pipe forming. In the case of the steel pipe, the hydrogen content varies around the circumferential direction and the specimen from the 180° position shows slightly higher diffusible hydrogen contents than the specimen from the 90° position for specimens from both the 12 mm and 18 mm thick pipes.

Since the amount of diffusible hydrogen is greatly affected by the level of strain, the results can be explained by the variation in strain level depending on the pipe thickness. From a study on the effect of buckling strain in the piping process, Okatsu et al., have reported that more strain is induced with increasing t/D ratio when the steel sheet is rolled to make the pipe [6]. The t/D ratio is 0.024 for the 12 mm thick pipe and 0.035 for the 18 mm thick pipe. Even though it is hard to quantitatively measure the buckling strain, the results confirm that the 18 mm thick pipe has a higher amount of diffusible hydrogen due to the higher level of strain or higher t/D ratio and thus has a higher susceptibility to HIC.

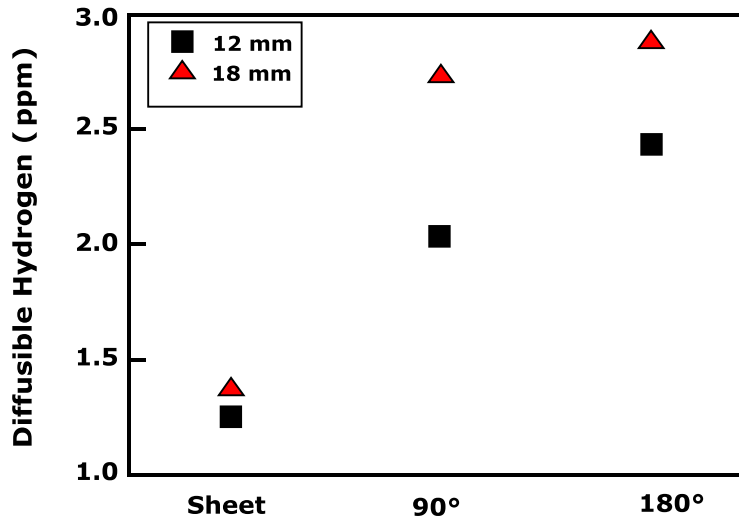


Figure 6. Content of diffusible hydrogen in the steel sheet and the steel pipe from the 90° and 180° positions after the HIC test.

In order to investigate the reasons for differences in the CAR values between coil and pipe, microstructural details were analyzed using EBSD (electron backscattered diffraction). Figure 7 shows kernel average misorientation maps from the 18 mm thick sheet and pipe. From the kernel average misorientation maps, an increase in dislocation density is confirmed after pipe forming.

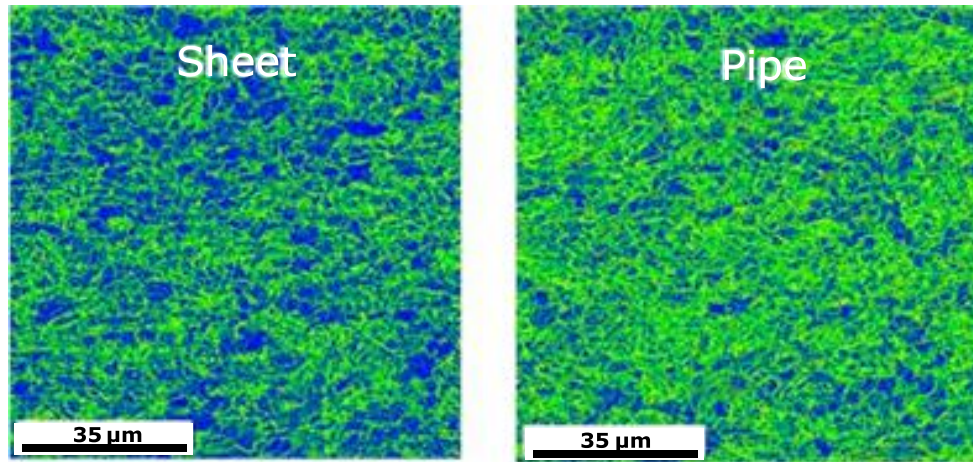


Figure 7. EBSD results of sheet and pipe with 18 mm thickness; Kernel average misorientation maps of sheet and pipe.

The higher diffusible hydrogen content of the pipes could be confirmed from results of hydrogen permeation tests, as well as by the glycerin method. Table III shows calculated hydrogen diffusion parameters of effective diffusivity, permeability and apparent solubility calculated after performing hydrogen permeation tests with a typically modified Devanathan-Stachurski cell [7].

Table III. Hydrogen Diffusion Parameters of Sheets and Pipes for Three X80 Coils

Hydrogen parameters	12 mm thickness			18 mm thickness		
	Sheet	Pipe 90°	Pipe 180°	Sheet	Pipe 90°	Pipe 180°
$D_{app}$ ( $\times 10^{-9}$ m <sup>2</sup> /s)	0.56	0.32	0.25	0.56	0.32	0.23
$J_{ss}L$ ( $\times 10^{-8}$ mol/m·s)	2.20	2.28	2.43	2.16	2.24	2.21
$C_{app}$ ( $\times 10$ mol/m <sup>3</sup> )	3.93	7.03	9.81	3.88	6.93	9.53

\*  $J_{ss}L$ : permeability,  $D_{app}$ : effective diffusivity,  $C_{app}$ : apparent solubility

It is clearly shown that the HIC susceptibility is closely related to the apparent hydrogen solubility ( $C_{app}$ ) which is greatly dependent upon the level of strain in the steel. The level of strain increases as the  $t/D$  ratio is increased and thus the HIC is more pronounced in the 18 mm thick pipe than in the 12 mm thick pipe. Additionally, the size of the inclusion cluster and individual inclusions also affects the HIC susceptibility and as shown the higher distribution of coarse inclusions is detected in the 18 mm thick material compared with the 12 mm thick steel. The hydrogen diffusion data also clearly demonstrate that the level of strain is higher at the 180° circumferential position than at the 90° position.

## Conclusions

1. High strength linepipe hot coils for sour environment were manufactured through mill trial production at POSCO. Strength and toughness of the produced hot coil met the requirements of API X80 grade. Sour service resistance was very good. No cracks were observed after HIC and 4-point bend beam testing.
2. The changes of yield strength after pipe forming depend on the pipe size. In the case of lower t/D ratios, the yield strength of the pipe was lower than that of the sheet because of the Bauschinger effect.

On the other hand, for higher t/D values, pipe yield strength is increased by pipe forming because the work hardening effect is larger than the Bauschinger effect.

3. The HIC resistance after pipe forming also depends on the pipe size. The HIC susceptibility increases as the t/D ratio is increased since the level of strain is increased. This deterioration can be explained by an increased amount of diffusible hydrogen after pipe forming. Through the hydrogen permeation test, it can be clearly seen that the effective diffusion coefficient ( $D_{app}$ ) is decreased while the apparent solubility ( $C_{app}$ ) is increased as the level of strain increased.

## References

1. EPA-453/R-93 045 (Environmental Protection Agency), "Report to Congress on Hydrogen Sulfide Air Emissions Associated with the Extraction of Oil and Natural Gas," October 1993, III-4.
2. M. Kimura et al., *Corrosion (NACE)*, 55 (1999), 756.
3. NACE Committee (2003), Review of Published Literature on Wet H<sub>2</sub>S Cracking of Steels Through 1989, NACE International, Houston, Texas.
4. R.J. Pargeter, *Corrosion (NACE)* 2007, March 11-15, Nashville, Tennessee, USA, Paper 07115.
5. NACE Standard TM0284 (2005), "Evaluation of Pipeline and Pressure Vessel Steels for Resistance to Hydrogen Induced Cracking" (Houston, TX: NACE International).
6. M. Okatsu, N. Shikanai and J. Kondo, *JFE GIHO*, 17 (2007), 20-25.
7. M.A.V. Devanathan and Z. Stachurski, *Journal of the Electrochemical Society*, 111 (1964), 619.